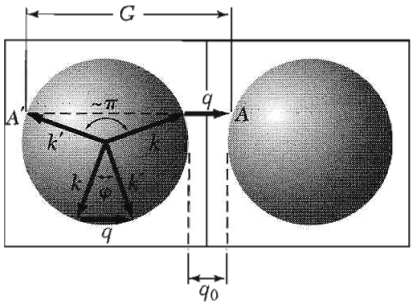

Figure 13 Two Fermi spheres in adjacent zones: a construction to show the role of phonon umklapp processes in electrical resistivity.

than in a normal electron-phonon scattering process at low temperatures. (In an umklapp process the wavevector of one particle may be "flipped over.")

Consider a section perpendicular to [100] through two adjacent Brillouin zones in bcc potassium, with the equivalent Fermi spheres inscribed within each (Fig. 13). The lower half of the figure shows the normal electron-phonon collision $\mathbf{k}' = \mathbf{k} + \mathbf{q}$, while the upper half shows a possible scattering process $\mathbf{k}' = \mathbf{k} + \mathbf{q} + \mathbf{G}$ involving the same phonon and terminating outside the first Brillouin zone, at the point A. This point is exactly equivalent to the point A' inside the original zone, where AA' is a reciprocal lattice vector $\mathbf{G}$. This scattering is an umklapp process, in analogy to phonons. Such collisions are strong scatterers because the scattering angle can be close to π.

When the Fermi surface does not intersect the zone boundary, there is some minimum phonon wavevector q_0 for umklapp scattering. At low enough temperatures the number of phonons available for umklapp scattering falls as $\exp(-\theta_U/T)$, where θ_U is a characteristic temperature calculable from the geometry of the Fermi surface inside the Brillouin zone. For a spherical Fermi surface with one electron orbital per atom inside the bcc Brillouin zone, one shows by geometry that $q_0 = 0.267\, k_F$.

The experimental data (Fig. 12) for potassium have the expected exponential form with $\theta_U = 23$ K compared with the Debye $\theta = 91$ K. At the very lowest temperatures (below about 2 K in potassium) the number of umklapp processes is negligible and the lattice resistivity is then caused only by small angle scattering, which is the normal (not umklapp) scattering.

MOTION IN MAGNETIC FIELDS

By the arguments of (39) and (41) we are led to the equation of motion for the displacement $\delta\mathbf{k}$ of a Fermi sphere of particles acted on by a force $\mathbf{F}$ and by friction as represented by collisions at a rate $1/\tau$:

$$\hbar\left(\frac{d}{dt} + \frac{1}{\tau}\right)\delta\mathbf{k} = \mathbf{F} \ . \tag{48}$$

The free particle acceleration term is $(\hbar d/dt)\,\delta\mathbf{k}$ and the effect of collisions (the friction) is represented by $\hbar\delta\mathbf{k}/\tau$, where τ is the collision time.

Consider now the motion of the system in a uniform magnetic field **B**. The Lorentz force on an electron is

(CGS) $$\mathbf{F} = -e\left(\mathbf{E} + \frac{1}{c}\mathbf{v}\times\mathbf{B}\right); \tag{49}$$

(SI) $$\mathbf{F} = -e(\mathbf{E} + \mathbf{v}\times\mathbf{B})$$

If $m\mathbf{v} = \hbar\delta\mathbf{k}$, then the equation of motion is

(CGS) $$m\left(\frac{d}{dt} + \frac{1}{\tau}\right)\mathbf{v} = -e\left(\mathbf{E} + \frac{1}{c}\mathbf{v}\times\mathbf{B}\right). \tag{50}$$

An important situation is the following: let a static magnetic field **B** lie along the z axis. Then the component equations of motion are

(CGS) $$m\left(\frac{d}{dt} + \frac{1}{\tau}\right)v_x = -e\left(E_x + \frac{B}{c}v_y\right);$$

$$m\left(\frac{d}{dt} + \frac{1}{\tau}\right)v_y = -e\left(E_y - \frac{B}{c}v_x\right); \tag{51}$$

$$m\left(\frac{d}{dt} + \frac{1}{\tau}\right)v_z = -eE_z.$$

The results in SI are obtained by replacing c by 1.

In the steady state in a static electric field the time derivatives are zero, so that the drift velocity is

$$v_x = -\frac{e\tau}{m}E_x - \omega_c\tau v_y; \qquad v_y = -\frac{e\tau}{m}E_y + \omega_c\tau v_x; \qquad v_z = -\frac{e\tau}{m}E_z, \tag{52}$$

where $\omega_c = eB/mc$ is the **cyclotron frequency,** as discussed in Chapter 8 for cyclotron resonance in semiconductors.

Hall Effect

The Hall field is the electric field developed across two faces of a conductor, in the direction $\mathbf{j}\times\mathbf{B}$, when a current **j** flows across a magnetic field **B**. Consider a rod-shaped specimen in a longitudinal electric field E_x and a transverse magnetic field, as in Fig. 14. If current cannot flow out of the rod in the y direction we must have $\delta v_y = 0$. From (52) this is possible only if there is a transverse electric field

(CGS) $$E_y = -\omega_c\tau E_x = -\frac{eB\tau}{mc}E_x; \tag{53}$$

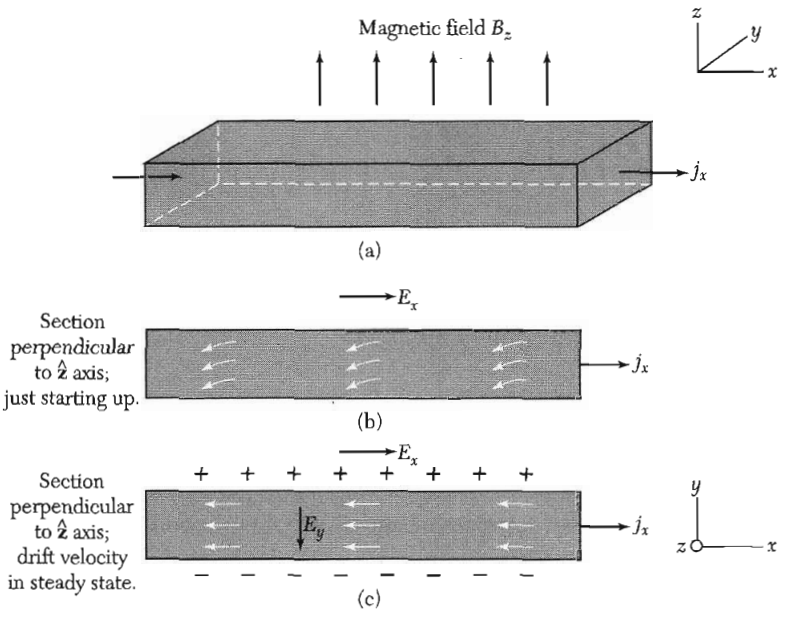

Figure 14 The standard geometry for the Hall effect: a rod-shaped specimen of rectangular cross-section is placed in a magnetic field B_z, as in (a). An electric field E_x applied across the end electrodes causes an electric current density j_x to flow down the rod. The drift velocity of the negatively-charged electrons immediately after the electric field is applied as shown in (b). The deflection in the $-y$ direction is caused by the magnetic field. Electrons accumulate on one face of the rod and a positive ion excess is established on the opposite face until, as in (c), the transverse electric field (Hall field) just cancels the Lorentz force due to the magnetic field.

(SI) $$E_y = -\omega_c \tau E_x = -\frac{eB\tau}{m} E_x \ .$$

The quantity defined by

$$\boxed{R_H = \frac{E_y}{j_x B}} \tag{54}$$

is called the **Hall coefficient**. To evaluate it on our simple model we use $j_x = ne^2\tau E_x/m$ and obtain

(CGS) $$R_H = -\frac{eB\tau E_x/mc}{ne^2\tau E_x B/m} = -\frac{1}{nec} \ ; \tag{55}$$

(SI) $$R_H = -\frac{1}{ne} \ .$$

This is negative for free electrons, for e is positive by definition.

Table 4 Comparison of observed Hall coefficients with free electron theory

[The experimental values of R_H as obtained by conventional methods are summarized from data at room temperature presented in the Landolt-Bornstein tables. The values obtained by the helicon wave method at 4 K are by J. M. Goodman. The values of the carrier concentration n are from Table 1.4 except for Na, K, Al, In, where Goodman's values are used. To convert the value of R_H in CGS units to the value in volt-cm/amp-gauss, multiply by 9×10^{11}; to convert R_H in CGS to m^3/coulomb, multiply by 9×10^{13}.]

Metal	Method	Experimental R_H, in 10^{-24} CGS units	Assumed carriers per atom	Calculated $-1/nec$, in 10^{-24} CGS units
Li	conv.	−1.89	1 electron	−1.48
Na	helicon	−2.619	1 electron	−2.603
	conv.	−2.3		
K	helicon	−4.946	1 electron	−4.944
	conv.	−4.7		
Rb	conv.	−5.6	1 electron	−6.04
Cu	conv.	−0.6	1 electron	−0.82
Ag	conv.	−1.0	1 electron	−1.19
Au	conv.	−0.8	1 electron	−1.18
Be	conv.	+2.7	—	—
Mg	conv.	−0.92	—	—
Al	helicon	+1.136	1 hole	+1.135
In	helicon	+1.774	1 hole	+1.780
As	conv.	+50.	—	—
Sb	conv.	−22.	—	—
Bi	conv.	−6000.	—	—

The lower the carrier concentration, the greater the magnitude of the Hall coefficient. Measuring R_H is an important way of measuring the carrier concentration. *Note:* The symbol R_H denotes the Hall coefficient (54), but the same symbol is sometimes used with a different meaning, that of Hall resistance in two-dimensional problems.

The simple result (55) follows from the assumption that all relaxation times are equal, independent of the velocity of the electron. A numerical factor of order unity enters if the relaxation time is a function of the velocity. The expression becomes somewhat more complicated if both electrons and holes contribute to the conductivity.

In Table 4 observed values of the Hall coefficient are compared with values calculated from the carrier concentration. The most accurate measurements are made by the method of helicon resonance which is treated as a problem in Chapter 14.

The accurate values for sodium and potassium are in excellent agreement with values calculated for one conduction electron per atom, using (55).

Notice, however, the experimental values for the trivalent elements aluminum and indium: these agree with values calculated for one *positive* charge carrier per atom and thus disagree in magnitude and sign with values calculated for the expected three negative charge carriers.

The problem of an apparent positive sign for the charge carriers arises also for Be and As, as seen in the table. The anomaly of the sign was explained by Peierls (1928). The motion of carriers of apparent positive sign, which Heisenberg later called "holes," cannot be explained by a free electron gas, but finds a natural explanation in terms of the energy band theory to be developed in Chapters 7–9. Band theory also accounts for the occurrence of very large values of the Hall coefficient, as for As, Sb, and Bi.

THERMAL CONDUCTIVITY OF METALS

In Chapter 5 we found an expression $K = \frac{1}{3}Cv\ell$ for the thermal conductivity of particles of velocity v, heat capacity C per unit volume, and mean free path ℓ. The thermal conductivity of a Fermi gas follows from (36) for the heat capacity, and with $\epsilon_F = \frac{1}{2}mv_F^2$:

$$K_{el} = \frac{\pi^2}{3} \cdot \frac{nk_B^2T}{mv_F^2} \cdot v_F \cdot \ell = \frac{\pi^2 nk_B^2 T\tau}{3m} \ . \tag{56}$$

Here $\ell = v_F\tau$; the electron concentration is n, and τ is the collision time.

Do the electrons or the phonons carry the greater part of the heat current in a metal? In pure metals the electronic contribution is dominant at all temperatures. In impure metals or in disordered alloys, the electron mean free path is reduced by collisions with impurities, and the phonon contribution may be comparable with the electronic contribution.

Ratio of Thermal to Electrical Conductivity

The **Wiedemann-Franz law** states that for metals at not too low temperatures the ratio of the thermal conductivity to the electrical conductivity is directly proportional to the temperature, with the value of the constant of proportionality independent of the particular metal. This result was important in the history of the theory of metals, for it supported the picture of an electron gas as the carrier of charge and energy. It can be explained by using (43) for σ and (56) for K:

$$\frac{K}{\sigma} = \frac{\pi^2 k_B^2 Tn\tau/3m}{ne\tau^2/m} = \frac{\pi^2}{3}\left(\frac{k_B}{e}\right)^2 T \ . \tag{57}$$